This article was downloaded by:
On: *14 January 2011*
Access details: *Access Details: Free Access*
Publisher *Taylor & Francis*
Informa Ltd Registered in England and Wales Registered Number: 1072954 Registered office: Mortimer House, 37-41 Mortimer Street, London W1T 3JH, UK

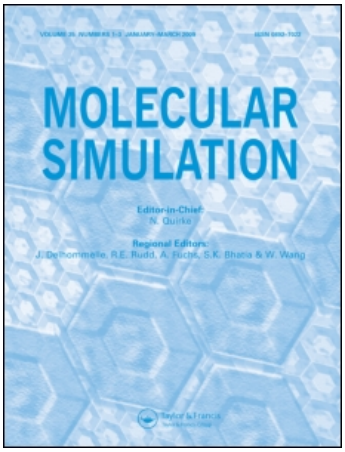

Molecular Simulation
Publication details, including instructions for authors and subscription information:
http://www.informaworld.com/smpp/title~content=t713644482

Characterisation of the effect of electrostatic interaction on the structure of Trp-cage using molecular dynamics simulation

Xiaoyu Wu[a]; Ganesan Narsimhan[a]
[a] Biochemical and Food Process Engineering, Department of Agricultural and Biological Engineering, Purdue University, West Lafayette, IN, USA

Online publication date: 24 November 2010

To cite this Article Wu, Xiaoyu and Narsimhan, Ganesan(2010) 'Characterisation of the effect of electrostatic interaction on the structure of Trp-cage using molecular dynamics simulation', Molecular Simulation, 36: 13, 1086 — 1095
To link to this Article: DOI: 10.1080/08927022.2010.504774
URL: http://dx.doi.org/10.1080/08927022.2010.504774

PLEASE SCROLL DOWN FOR ARTICLE

Full terms and conditions of use: http://www.informaworld.com/terms-and-conditions-of-access.pdf

This article may be used for research, teaching and private study purposes. Any substantial or systematic reproduction, re-distribution, re-selling, loan or sub-licensing, systematic supply or distribution in any form to anyone is expressly forbidden.

The publisher does not give any warranty express or implied or make any representation that the contents will be complete or accurate or up to date. The accuracy of any instructions, formulae and drug doses should be independently verified with primary sources. The publisher shall not be liable for any loss, actions, claims, proceedings, demand or costs or damages whatsoever or howsoever caused arising directly or indirectly in connection with or arising out of the use of this material.

Molecular Simulation
Vol. 36, No. 13, November 2010, 1086–1095

Taylor & Francis
Taylor & Francis Group

Characterisation of the effect of electrostatic interaction on the structure of Trp-cage using molecular dynamics simulation

Xiaoyu Wu and Ganesan Narsimhan*

Biochemical and Food Process Engineering, Department of Agricultural and Biological Engineering, Purdue University, West Lafayette, IN 47907, USA

(*Received 19 April 2010; final version received 22 June 2010*)

A mutated variant of 20 amino acid miniprotein Trp-cage (TC5b), called TC5c (Asp9 replaced by Asn9), was designed to demonstrate the effect of a salt bridge. As a result of strong electrostatic interaction, the distance distribution between Asp9 and Arg16 exhibited a larger probability in the range of the salt bridge for TC5b compared to TC5c. The probability of α-helix formation for residues 3–8, as well as for residues 11–14, was high for TC5b. The salt bridge formation between Asp9 and Arg16 in TC5b was indicated by (a) a strong correlation of their distance of separation with the subtended angle with the centre and (b) a step decrease in the distance between Gly11O and Arg16H at 12 ns. Replica exchange molecular dynamics simulation at different temperatures in the range of 270–590 K indicated that the average distance between Asp9 and Arg16, end-to-end distance, root mean square deviation with respect to a reference NMR structure of TC5b did not change significantly with temperature below 370 K for TC5b and increased at higher temperatures. These values were higher for TC5c for the whole temperature range, with their rate of increase with temperature being higher below 370 K.

Keywords: Trp-cage; molecular dynamics; AMBER; protein folding; salt bridge

Downloaded At: 17:03 14 January 2011

Introduction

The 20 amino acid miniprotein Trp-cage TC5b (NLYIQWLKDG GPSSGRPPPS) optimised by the Andersen group is currently the smallest protein with a stable compact structure in solution [1]. It contains a short α-helix in residues 2–8, followed by a single 3_{10}-helix turn in residues 11–14 and a C-terminal polyproline II helix to pack back along the helical axis to enwrap the central tryptophan (Trp6) in the hydrophobic core. Helical N-capping residues and a solvent-exposed salt bridge (Asp9–Arg16) are supposed to strengthen the stability of the Trp-cage structure and may also result in a high cooperativity during the folding pathway [2]. Experimental techniques, such as CD, fluorescence and chemical shift deviations, have successfully elucidated the thermal denaturation profiles of the protein, which definitely shows that TC5b possesses protein-like features [1–5]. This small miniprotein folds spontaneously very fast into a Trp-cage structure in around 4 μs [6], within a time range for a molecular dynamics (MD) simulation. Thus, all the features that TC5b possesses, such as small size, ultrafast folding rate and protein-like structure, make it an ideal model system for folding simulations.

TC5b has been chosen as a candidate for simulation by many research groups because of its good properties. These simulation research works have obtained their folding properties, such as equilibrium structure and thermal stability, via different theoretical methods: all-atom or coarse-grained; implicit solvent or explicit solvent; different force fields (AMBER, CHARMM, OPLS, etc.) [7–15]. In addition, some of the results are in good agreement with the experimental findings. The effect of the salt bridge on hydrophobic core formation in Trp-cage was investigated [7] and shown that these hydrophobic cores were separated by a salt bridge between Asp9 and Arg16 in the intermediate state. In this paper, we focus on the influence of the salt bridge (Asp9 and Arg16) on the folding pathway of Trp-cage since it plays an important role in this pathway. Therefore, it is of interest to find how the modification of intrachain interactions by the mutation of Asp9 or Arg16 (TC5c) affect the stability and folding rate of Trp-cage. We choose Asp9 to be mutated by Asn9 based on the following reasons: (1) Asn has less charge, which will reduce the salt bridge interaction. (2) The difference between these two amino acids (Asp and Asn) is only in the replacement of the carboxylate $C(=O)O^-$ group by the amide $C(=O)NH_2$ group (Asn), as shown in Figure 1(a), which should have little effect on the whole spatial arrangement of this small polypeptide, and does not change the length of the side chain of the ninth amino acid. In order to overcome the possibility of Trp-cage being trapped in local minima and to increase the sampling efficiency, replica exchange molecular dynamics (REMD) simulation [16] was employed for both TC5b and TC5c simulations.

*Corresponding author. Email: narsimha@purdue.edu

ISSN 0892-7022 print/ISSN 1029-0435 online
© 2010 Taylor & Francis
DOI: 10.1080/08927022.2010.504774
http://www.informaworld.com

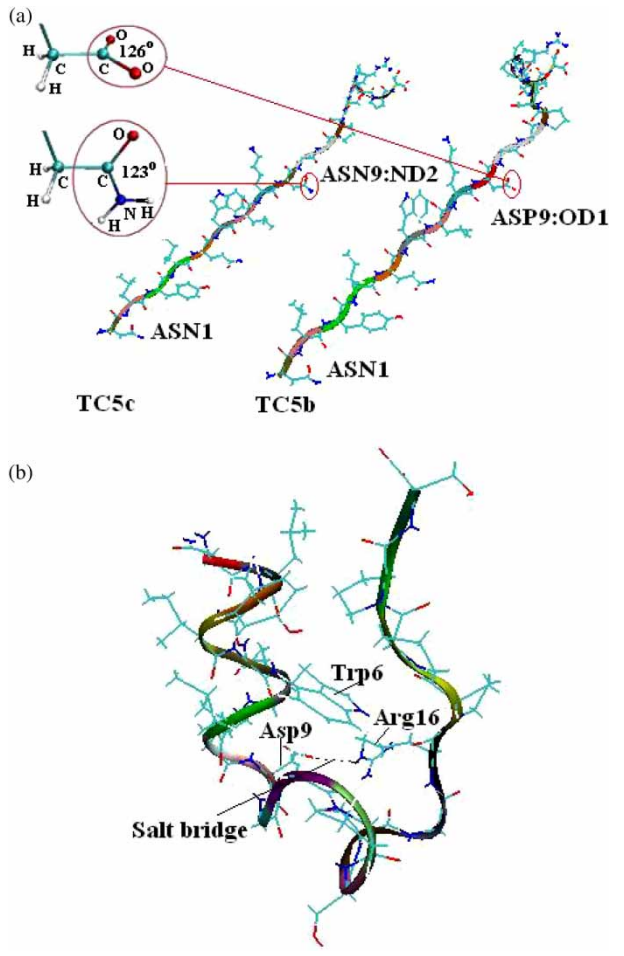

Figure 1. (a) Comparison of the initial fully extended structures of Trp-cage between the native (TC5b) and the mutant (TC5c). The top left shows the amplified picture of the side chain of Asp9 (TC5b) and Asn9 (TC5c), respectively. (b) The NMR folded structure of Trp-cage (PDB code: 1L2Y, the first structure of the total 38 NMR structures).

Method

All the simulations were run using AMBER 10 program [17], where the AMBER ff99 force field [18] was employed, with the exception of Φ/Ψ dihedral parameters which were refitted [9]. The initial linear structures of TC5b (NLYIQWLKDG GPSSGRPPPS) and TC5c (NLYIQWLKNG GPSSGRPPPS) were built up by the Leap module included in AMBER 10.0 package (Figure 1(a)). Minimisation of the structure to remove bad contact and steric hindrances was performed for 1000 steps before starting the MD calculations. Both classical MD simulation and REMD simulation were employed. Three different temperatures (325, 415 and 570 K) were chosen for the classical MD simulation. At constant temperature, the MD simulations were fully unrestrained in a canonical ensemble using Sander module and separated into two stages. In the first stage, a 50 ps calculation with a 0.5 fs time step was performed as the system was slowly heated up to a target temperature at a 1 ps coupling constant for temperature control [19]. Following the first heating stage, a 900 ns simulation with a 2 fs time step was run at a target temperature with a 1 ps coupling constant [7,9,20].

The GB/SA implicit solvent model was employed to incorporate the solvent effect [21,22]. Even though it has been suggested that the use of the GB/SA model for an implicit solvent could overestimate salt bridge formation [23,24], GB/SA model predictions of the Trp-cage structure have been found to agree well with experiments [9]. As will be shown later, this is consistent with root mean square deviation (RMSD) values between the MD simulation and the NMR structure reported here. In addition, the effect of the lowering of the dielectric constant due to charge density in the vicinity of protein is expected to be small since Trp-cage possesses only two charges.

The trajectories of the simulation were collected for every 1 ps. For the REMD simulation, 16 replicas were used with temperatures of 269.5, 285.5, 300.0, 316.5, 334.0, 351.0, 371.8, 391.0, 413.9, 435.0, 460.7, 485.0, 512.9, 535.9, 570.9 and 595.2 K, respectively. Neighbour lists were utilised and updated every 2.5 fs. Also, neighbour lists were utilised and updated every fifth integration step. Constraints were used for bond lengths using the LINCS algorithm for the protein [25]. All simulations and analysis were performed using AMBER and VMD software.

To illustrate the folding pathway of Trp-cage, the following order parameters were analysed using the following modules in AMBER 10.0 package: potential energy, root-mean-square deviation (RMSD), radius of gyration (RG), end-to-end distance, content of α-helix, fraction of native contacts and interstrand hydrogen bonds. Most of the plots were drawn by Xmgr software except the 3D structures of TC5b, TC5c and the NMR data, which were created by VMD software [26].

Results and discussion

Comparison of the initial extended structures of TC5b and TC5c

Trp-cage native type (TC5b) and its mutant (TC5c) were employed to test the effect of the electrostatic interaction on the folding pathway of Trp-cage, in which Asp in the ninth sequence in TC5b was replaced by Asn in the same position of TC5c (sequences of TC5b and TC5c are shown in the Method section). The difference between them is based only on one amino acid, which is supposed to reduce the original electrostatic interaction between Asp9 and Arg16 after the oxygen atom in the side chain of Asp9 (TC5b) is replaced by the nitrogen atom in the side chain of the Asn9 (TC5c). The replacement of Asp9 (TC5b) by Asn9 (TC5c) decreased the stability of the molecular structure due to the loss of the electrostatic interaction. In addition, it also offsets the stability of the structure by increasing the hydrophobicity inside its core.

Downloaded At: 17:03 14 January 2011

The initial fully extended structures for these two types of Trp-cage (TC5b and TC5c) are shown in Figure 1(a). In addition to the different types of atoms in the side chain (Asp9 as opposed to Asn9), it was also observed from Figure 1(a) that these atoms were located at different positions: the angle of OD1—CG—ND2 (123°, Asn9) is smaller than the angle of OD1—CG—OD2 (126°, Asp9) due to less repulsion between O and N than O and O. Since the initial structure built up by the Xleap module may have steric clashes, a short minimisation for the starting structure was executed to remove the bad contacts before starting MD.

Figure 1(b) shows the NMR structure of TC5b (PDB code: 1L2Y), which possesses typical features of a stable globular structure of a protein. This NMR structure is also chosen as a reference structure to be compared with the lowest energy structure of TC5b and TC5c obtained by the simulation.

Pair comparison among the 3D structures of TC5b and TC5c at the lowest free energy from the simulation and the NMR structure of TC5b

The averages of 1000 structures around the lowest energy structure over 1 ns were defined as the equilibrium structure. The comparison shown in Figure 2 was based on the RMSD calculation of heavy atoms in the whole backbone (excluding the terminal amino acids since these two amino acids have a poor definition in the NMR structure), as shown in Figure 2(a)–(c). Although the

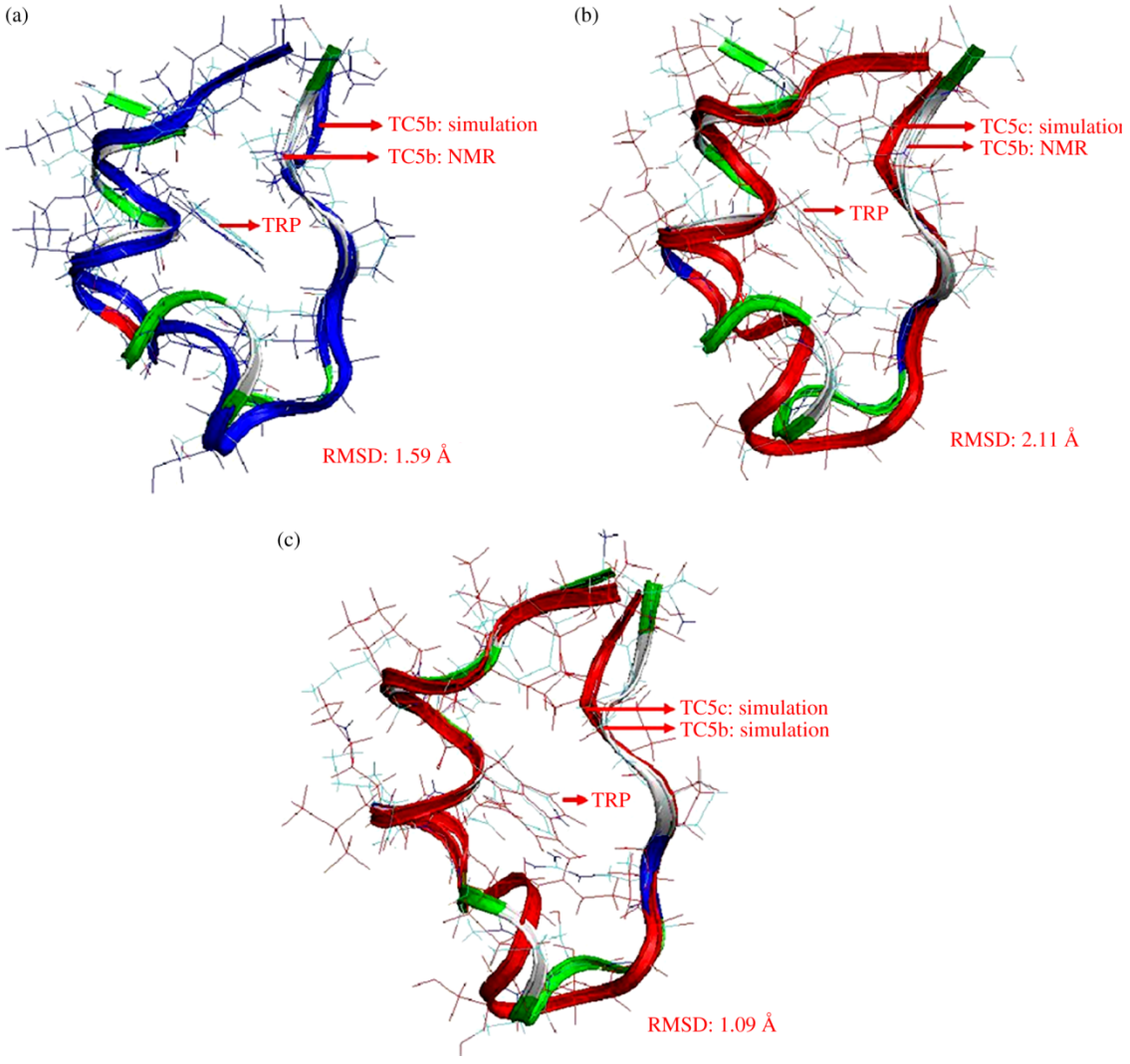

Figure 2. Comparison of the lowest energy structures obtained by simulation with the NMR structure: (a) RMSD comparison of the simulated TC5b structure and NMR TC5b structure along the whole backbone (except two terminal amino acids); (b) RMSD comparison of the simulated TC5c structure and NMR TC5b structure along the whole backbone (except two terminal amino acids) and (c) RMSD comparison of the simulated TC5b structure and simulated TC5c structure along the whole backbone (except two terminal amino acids).

Downloaded At: 17:03 14 January 2011

Downloaded At: 17:03 14 January 2011

NMR structure of TC5c (the difference between TC5b and TC5c is in the atoms that are located at the end of the side chains) is not available, making a RMSD comparison between TC5c and the NMR structure of TC5b will provide an insight into how the point mutation in the side chains would affect the overall conformational change.

Figure 2(a) shows the comparison of the equilibrium structure of TC5b with the NMR structure by overlapping the two centres of the whole backbone (excluding the two terminal amino acids). The RMSD value for the whole backbone (excluding the two terminal amino acids) between the MD structure and the NMR structure is only 1.59 Å, indicating similarity to the NMR structure. Both structures share the following features of a typical globular structure: the secondary structure contains an α-helix (residues 2–8), followed by a single turn of 3_{10}-helix present from residues 11 to 14 and a polyproline II helix formed in the C-terminal (residues 17–19); the compact hydrophobic core consists of the indole ring of Trp6 in the centre, flanked by the side chains of Tyr3, Leu7 and three proline residues (Pro12, Pro18 and Pro19); a salt bridge between Asp9 and Arg16 formed near the single turn of 3_{10}-helix is believed to help stabilise the compact structure. To investigate which region of these two types of structure is different, a subdivided RMSD comparison along the backbones was carried out, in which the backbones were separated by three different regions: residues 2–8 (α-helix region) residues 11–14 (3_{10}-helix region), and residues 15–19 (polyproline II helix region). The RMSD comparison of the MD and NMR structures based on the backbone extending from residues 2 to 8 shows a small value of 0.43 Å, which indicated that the α-helix structure of these seven residues obtained by MD simulation was very close to that of the NMR structure (shown in Figure 1A of the Supplementary Material, available online). The structural comparison based on the RMSD calculation of the other two regions (not shown here) gave values of 0.44 and 0.32 Å for a comparison on the 3_{10}-helix region (residues 11–14) and polyproline II helix region (residues 15–18), respectively. Thus, the RMSD/residue values for these three secondary structure domains are: 0.11 Å (3_{10}-helix) > 0.08 Å (polyproline II helix region) > 0.061 Å (α-helix). The 3_{10}-helix region for the MD structure is not as closely packed to the central hydrophobic core (a slight shift out of the core) as that for the native NMR structure (see Figure 2(a)).

Although the NMR structure of TC5b may be different from the NMR structure of the mutant (D9N) (it is not available now), it is currently the most stable structure for this protein family, and thus the NMR structure of TC5b is ideal to be chosen as the reference structure of the experimental model to be compared with TC5c. The overlap of the MD structure of TC5c and the NMR structure of TC5b (Figure 2(b)) shows that the backbone heavy-atom RMSD between these two species is around 2.11 Å. Although this value was higher than that between the MD structure of TC5b and the NMR structure (Figure 2(a)), it was much less than the generally defined RMSD value of 3.0 Å, above which an unfolded state is indicated. For TC5c, residues 2–8 form a short α-helix, followed by a single turn along residues 11–14, and the rest of the residues wraps back along the α-helix axis towards the N-terminus (Figure 3). This suggested that the mutant species formed a certain folded structure, which shared certain structural characteristics with the NMR structures. On the other hand, the mutant (TC5c) had a different structure compared to the NMR structure of TC5b, with the major deviation being around residues 11–14. It is apparent that residues 11–14 of TC5c did not form a 3_{10}-helix during the simulation, which was replaced by a big flat turn. The mutation of Asp9 by Asn9 (the carboxylate $C(=O)O^-$ group is replaced by the amide $C(=O)NH_2$ group at the end of the side chain) has a big effect on the interaction between neighbouring residues. For example, although the side chain of Trp6 in TC5c also formed the centre of the hydrophobic core, the ring of the side chain was a little closer to the side chain of Asn9 compared to Asp9 in TC5b because of higher non-polar interaction between the indole ring (Trp6) and NH_2 (Asn9) in TC5c. The movement of Gly11 in TC5b is restrained by the formation of the salt bridge (shown in Figure 4(a)), resulting in the formation of 3_{10}-helix. However, no 3_{10}-helix was observed in TC5c because Gly11 is more flexible due to the weak interaction between Asn9 and Arg16. The mutation in residue 9 also had a certain effect on the α-helix conformation from residues 2 to 8 (see Figure 1B of the Supplementary Material, available online), where the RMSD comparison of the MD structure of TC5c with the NMR structure is 0.70 Å, almost two times as that for the comparison of MD and NMR structures of TC5b (Figure 2(b)). The absence of the salt bridge between residues 9 and 16 in TC5c did not have any effect on the polyproline II helix formation (residues 15–19). A comparison of RMSD values for three different regions (residues 2–8, 11–14 and 15–19, respectively) between MD and NMR structures of TC5c revealed that the major deviation was in the 3_{10}-helix region (residues 11–14) and α-helix region (residues 2–8), as indicated by the RMSD/residue values of 0.15 Å (residues 11–14) and 0.10 Å (residues 2–8), respectively.

We also compared the MD structures of TC5b and TC5c as shown in Figure 2(c). The RMSD value for the whole backbone between these two species was only 1.09 Å, consistent with our previous observation that these two MD structures exhibited comparable 'folded' structures. The RMSD/residue for the α-helix region (residues 2–8) was quite small (0.061 Å), whereas the value for the 3_{10}-helix region (residues 11–14) was around 0.11 Å (see Figure 1C of the Supplementary Material, available online), consistent with our previous finding that the major difference between the two lies in the formation of the 3_{10}-helix region.

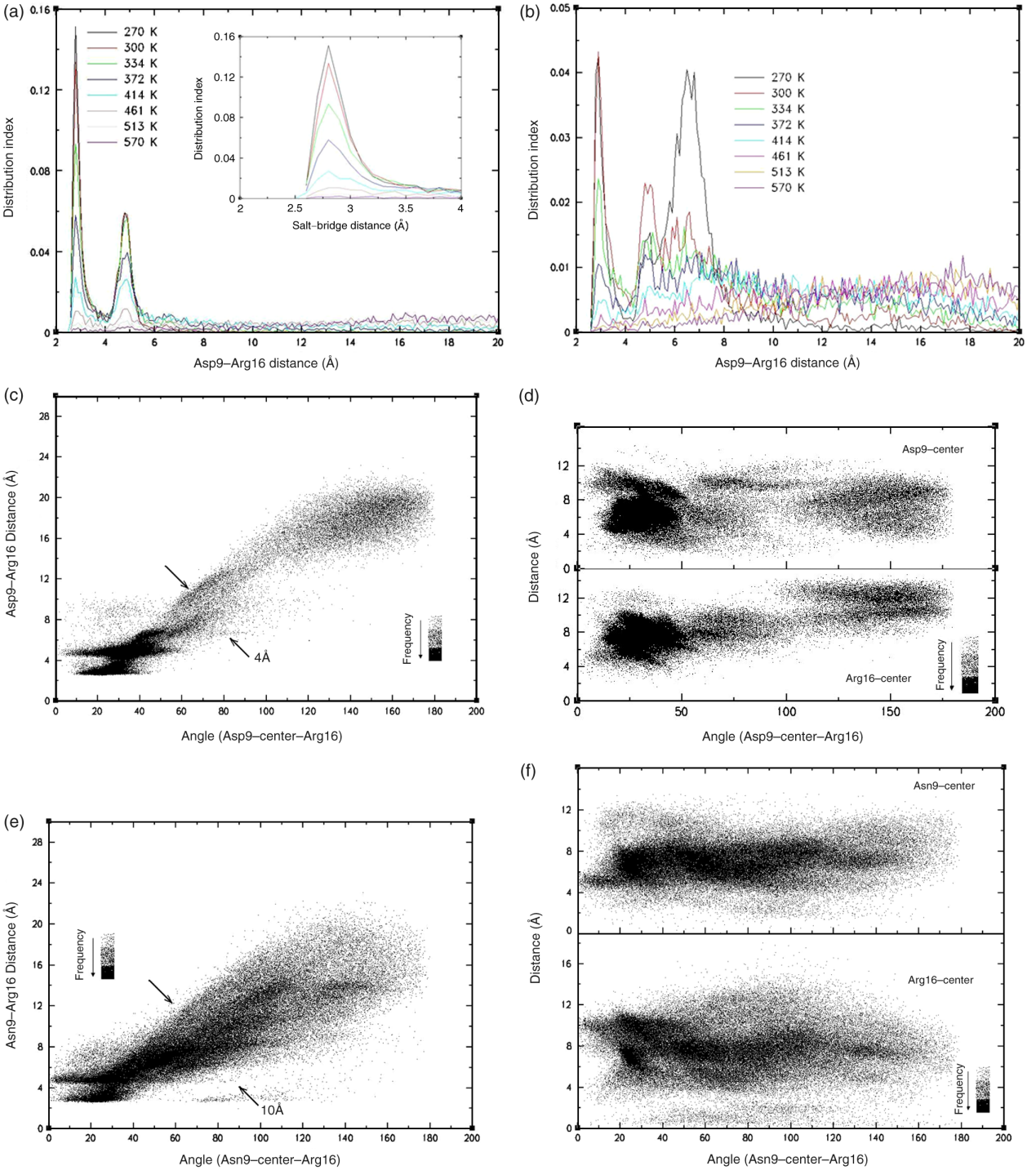

Figure 3. Comparison of the parameters for the salt bridge of TC5b and TC5c. (a) Distribution of the distance between Asp9 and Arg16 (salt bridge) during the simulation at different temperatures for TC5b. The inset gives the same plot on an expanded scale for different temperatures around the distance of 2.8 Å. (b) Distribution of the distance between Asn9 and Arg16 during the simulation at different temperatures for TC5c. (c) Distance of Asp9–Arg16 vs. the angle of Asp9–centre–Arg16 for TC5b. Higher point density represents higher frequency. (d) (Upper) distance of Asp9–centre of the molecular structure for TC5b vs. the angle of Asp9–centre–Arg16; (lower) distance of Arg16–centre of the molecular structure for TC5b vs. the angle of Asp9–centre–Arg16. (e) Distance of Asn9–Arg16 vs. the angle of Asn9–centre–Arg16 for TC5c. Higher point density represents higher frequency. (f) (Upper) distance of Asn9–centre of the molecular structure for TC5c vs. the angle of Asn9–centre–Arg16; (lower) distance of Arg16–centre of the molecular structure for TC5c vs. the angle of Asn9–centre–Arg16.

Downloaded At: 17:03 14 January 2011

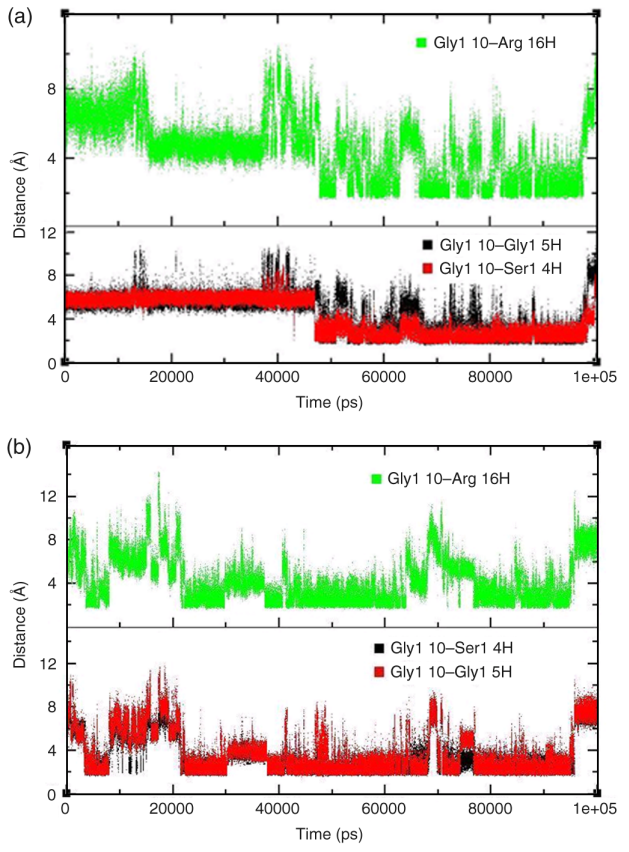

Figure 4. Comparison of the distance of the hydrogen bond near the 3_{10}-helix region as a function of time for TC5b and TC5c: (a) distance of Gly11-oxygen (O) and Ser14-hydrogen (H) (black line), distance of Gly11O and Ser14H (red line), and distance of Gly11O and Arg16H as a function of time for TC5b and; (b) distance of Gly11O and Ser14H (black line), distance of Gly11O and Ser14H (red line), and distance of Gly11O and Arg16H as a function of time for TC5c (colour online).

Comparison of the salt bridge change by the mutation in atomic details

The distribution of the distance between Asp9 and Arg16 (salt bridge) for all the structures during the simulation at different temperatures is shown for TC5b and TC5c in Figure 3(a) and (b), respectively. As can be seen from Figure 3(a), the distribution exhibits a large peak at around 2.8 Å and a much smaller peak at 5 Å at lower temperatures. As temperature increases, however, these peaks become less pronounced and the area under the distribution for larger distances increases. This suggests more unfolding of the molecule at higher temperatures. For TC5c, the distribution exhibits a much smaller peak at the same distance of 2.8 Å compared to that for TC5b. However, unlike TC5b, the second peak is not observed at the same distance. In addition, the area under the distribution at larger distances of separation is found to be much larger than that for TC5b. At higher temperatures, the distance becomes more random for TC5c. These results suggest that the salt bridge in TC5c is less stable than that in TC5b. To further explain the relationship between the interaction of the salt bridge and its position, we made the plots of *distance of the salt bridge*, *distance of Asp9O (or Asn9O) to the centre*, and *the distance of Arg16N to the centre* as a function of the angle of Asp9O (or Asn9O)–centre–Arg16N. Figure 3(c) shows that the distance of the salt bridge of TC5b has a strong linear correlation with the angle of Asp9–centre–Arg16 (the band width is around 4 Å), indicating that most of the change in the distance of the salt bridge is caused by the movement of Asp9O or Arg16N around the centre and not by the movement in and out of the centre. Furthermore, it was clearly shown in Figure 3(c) that a high density appeared in the region of a strong salt bridge formation with a small angle, suggesting that the salt bridge prefers to be stacked at a certain position after its formation. And this position is located near the surface of the molecular structure. This was also confirmed by Figure 3(d), which shows that the distance of Asp9O (Arg16N) to the centre was mostly packed in the range of around 7.5 Å with a small Asp9–centre–Arg16 angle (which are consistent with the RG value of around 7 Å). For comparison, similar plots are made for TC5c to explain how the movement of Asn9 and Arg16 changed if the electrostatic interaction between them was removed during the simulation. Figure 3(e) shows that the distance between Asn9 and Arg16 of TC5c has a weak linear correlation with the angle of Asn9–centre–Arg16 (the band width is around 10 Å), indicating that the change in the distance is mostly caused by the random movement of Asn9O or Arg16N from the centre. Another observation from Figure 3(e) is that the density of the distance between Asn9 and Arg16 has a much wider distribution (distance: 3–12 Å; angle: 0–120°) than that of TC5b (distance: 3–6 Å; angle: 0–50 °), which confirmed that the movement of Asn9O or Arg16N was more random and not limited by the interaction between Asn9 and Arg16. Figure 3(f) clearly shows that the distance of Asn9 (or Arg16) to the centre is almost independent of the angle between them and the high density of the distance is almost uniformly distributed in the angle range of 20–160°, indicating that the movement of these two amino acids is less constrained by the interaction between them.

Hydrogen bonds change by the mutation in atomic details

Two regions were selected for the target of the secondary structure analysis based on their distance to the mutated position and their own properties of the secondary structure: residues 2–9 (near the α-helix region) and residues 11–16 (near the 3_{10}-helix region). In our analysis, only the distance between the hydrogen atom and the

Downloaded At: 17:03 14 January 2011

oxygen atom in the backbone in these two regions was calculated since the secondary structure that is formed is related mostly to the arrangement of the backbone, and the hydrogen bonds from the backbone are the most important for this arrangement.

The comparison of structures for TC5b and TC5c in the region of residues 2–9 (see Figure 1C of the Supplementary Material, available online) indicates that the difference is not significant. Figure 4(a) shows the distance of Gly11O–Arg16H, Gly11O–Gly15H and Gly11O–Ser14H for TC5b as a function of time. It can be seen from the plot of the distance of Gly11O–Arg16H vs. time that the distance experienced two step decreases at around 12 and 48 ns. The first transition at 12 ns is consistent with the time of formation of the salt bridge. It is interesting to note that the time of the second transition (48 ns) coincides with the end time of large fluctuations for other parameters such as RMSD, RG and end-to-end distance (not shown here). The large fluctuation before the second transition coincides with a similar behaviour for

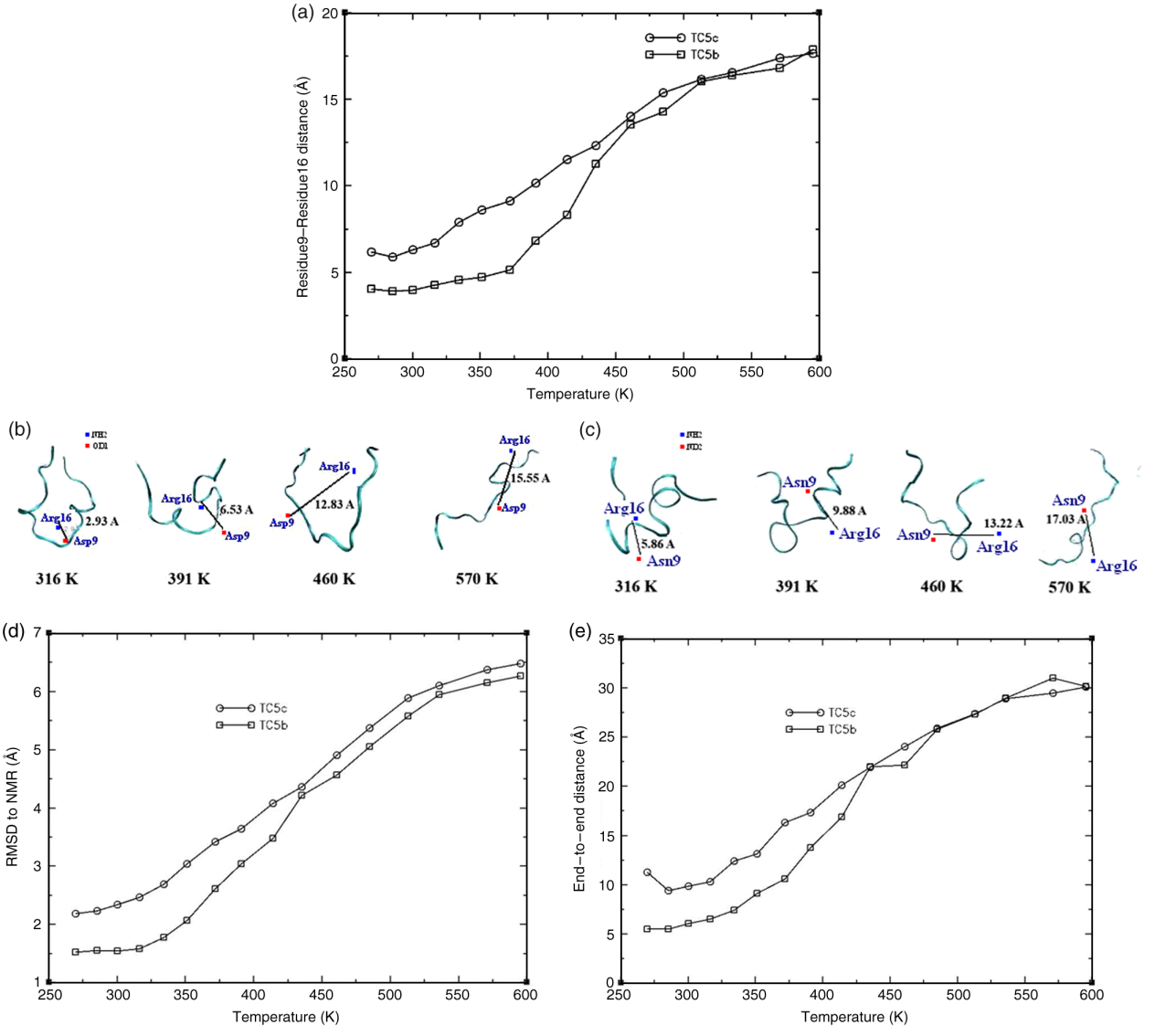

Figure 5. Effect of the temperature on the stability of TC5b and TC5c. (a) Comparison of the distance of residues 9 and 16 for the lowest energy structures of TC5b and TC5c as a function of temperature. (b) The lowest energy MD structures of TC5b at selected temperatures (316, 391, 460 and 570 K). The distance between Asp9 and Arg16 is indicated for each structure. (c) The lowest energy MD structures of TC5c at selected temperatures (316, 391, 460 and 570 K). The distance between Asn9 and Arg16 is indicated for each structure. (d) Comparison of the RMSD of the lowest energy MD structure of TC5b and TC5c with respect to the NMR structure of TC5b (reference) as a function of temperature. (e) Comparison of the end-to-end distance of the lowest energy states for TC5b and TC5c as a function of temperature. Here, the lowest energy state is defined as the average based on the 1000 lowest potential energy MD structure for every temperature during the simulation.

Downloaded At: 17:03 14 January 2011

RMSD, RG and end-to-end distance (see Figure 2 of the Supplementary Material, available online), suggesting that these fluctuations are predominantly due to the movement of Gly11 since the position of Arg16 was fixed due to the salt bridge as early as at 12 ns (see Figure 3 of the Supplementary Material, available online). The effect of

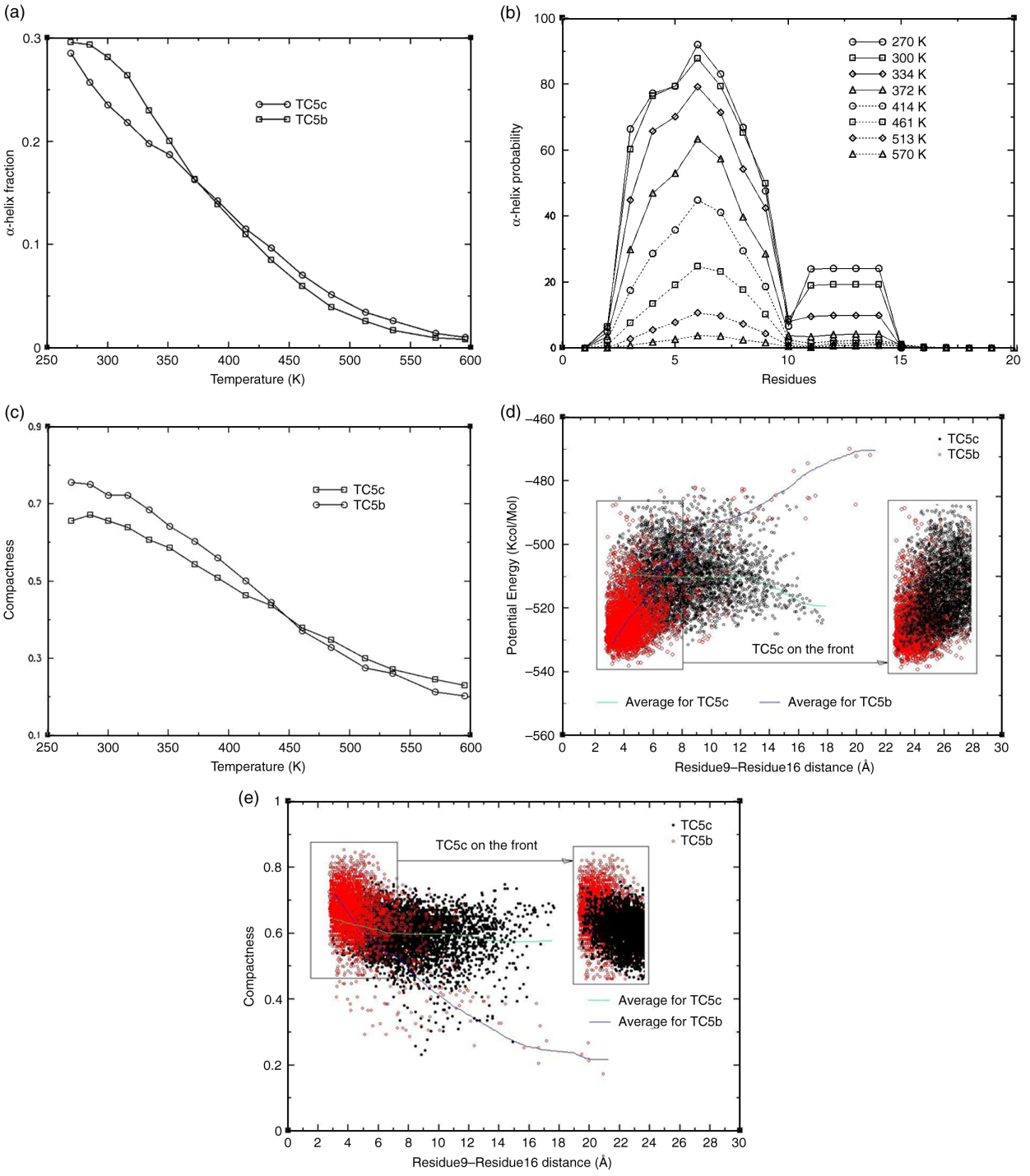

Figure 6. Effect of the temperature on the secondary and tertiary structures of TC5b and TC5c. (a) Comparison of the percentage of α-helix for TC5b and TC5c as a function of temperature. (b) The probability of α-helix formation for every residue for TC5b at different temperatures. (c) Comparison of the lowest energy compactness of TC5b and TC5c as a function of temperature. Here, the lowest energy state is defined as the average based on the 1000 lowest potential energy MD structure for every temperature during the simulation. (d) Potential energy vs. distance between residues 9 and 16 for TC5b and TC5c. (e) Compactness vs. distance between residues 9 and 16 for TC5b and TC5c. 'TC5c on the front' in (d) and (e) means that for the overlap region (left rectangle), an additional plot (right rectangle) is given, where the plot for TC5c is shown in the front of TC5b.

Downloaded At: 17:03 14 January 2011

the relocation of Gly11 was also supported by the plot of the distance of Gly11O–Gly15H, and the distance of Gly11O–Ser14H (lower panel of Figure 4(a)): both the distances have an apparent transition to a lower level at around 48 ns with a smaller fluctuation before the transition time. This also suggested that 3_{10}-helix (residues 11–14) may begin to be formed at this time. Figure 4(b) gives similar plots for TC5c as a comparison. TC5c did not exhibit transitions, indicating thereby that the movement of Gly11 is much more flexible and its movement is not limited as a result of the weak interaction between Asn9 and Arg16. Also, residues 11–14 are not in a stable 3_{10}-helix state, although the distance of Gly11O–Ser14H becomes sufficiently small at times, which may enable the formation of the hydrogen bond.

Thermal stability of TC5b and TC5c

Figure 5(a) gives the variation of average distance between Asp9 and Arg16 with temperature for TC5b and TC5c. Consistent with the earlier observation of the distribution of distance, the average distance increases with temperature. Also, the average distance is higher for TC5c, thus indicating that its salt bridge is less stable. The RMSD of the lowest energy MD (average of 1000 structures around the lowest energy state) structure of TC5b and TC5c compared to the NMR structure of TC5b (reference) are shown in Figure 5(d). Up to 320 K, the RMSD value for TC5b is around 1.5 Å and does not change with temperature. At higher temperatures, however, the RMSD value increases with temperature for both TC5b and TC5c. The RMSD values for TC5c were always found to be higher than that for TC5b. This difference is about 0.75 Å at lower temperatures (lower than 450 K) and decreases to about 0.25 Å at higher temperatures. Such a behaviour may be because the thermal energy is able to overcome the electrostatic interactions of the salt bridge for TC5b at higher temperatures. A similar behaviour is observed for the end-to-end distance (see Figure 5(c)). The percentage of α-helix is found to decrease with temperature for TC5b and TC5c, as shown in Figure 6(a), with the value for the former being higher; this difference in percentage of α-helix between TC5b and TC5c is higher at lower temperatures (below 350 K). Figure 6(b) shows the probability of α-helix formation for every residue for TC5b at different temperatures. The probability is high for residues 3–8 and 11–14, consistent with the NMR structure. The probability of α-helix formation decreases at higher temperatures. The variation of compactness (compared with the NMR structure of TC5b as explained in the Method section) with temperature is shown in Figure 6(c). The value for TC5b is higher than that for TC5c. Also, the compactness value decreases with temperature possibly due to unfolding of the molecule. These results indicate a strong correlation between the compactness and the salt bridge distance, as well as the potential energy.

Conclusions

TC5b is more stable than TC5c as shown by the analysis of the RMSD with respect to the NMR structure, compactness and the formation of the α-helix structure at different temperatures. Salt bridge is believed to be an important factor for the stabilisation of the structure of Trp-cage in that it strengthens the hydrophobic core by the strong electrostatic interaction on the surface. Also, salt bridge has an influence on the folding kinetics of Trp-cage by limiting the positions of Asp9 and Arg16, which affect other structural adjustment, such as formation of α-helix. The simulation results indicate the high likelihood of α-helix formation for residues 3–8 and 11–14 for both TC5b and TC5c, with this probability being higher for the former.

Acknowledgements

We would like to acknowledge the Purdue Research Foundation for providing financial support to X.W.

References

[1] J.W. Neidigh, R.M. Fesinmeyer, and N.H. Andersen, *Designing a 20-residue protein*, Nat. Struct. Biol. 9 (2002), pp. 425–430.
[2] P. Hudaky, P. Straner, V. Farkas, G. Varadi, G. Toth, and A. Perczel, *Cooperation between a salt bridge and the hydrophobic core triggers fold stabilization in a Trp-cage miniprotein*, Biochemistry 47 (2008), pp. 1007–1016.
[3] Z. Ahmed, I.A. Beta, A.V. Mikhonin, and S.A. Asher, *UV-resonance Raman thermal unfolding study of Trp-cage shows that it is not a simple two-state miniprotein*, J. Am. Chem. Soc. 127 (2005), pp. 10943–10950.
[4] A.T. Iavarone, A. Patriksson, D. van der Spoel, and J.H. Parks, *Fluorescence probe of Trp-cage protein conformation in solution and in gas phase*, J. Am. Chem. Soc. 129 (2007), pp. 6726–6735.
[5] M.R. Bunagan, X. Yang, J.G. Saven, and F. Gai, *Ultrafast folding of a computationally designed Trp-cage mutant: Trp2-cage*, J. Phys. Chem. B 110 (2006), pp. 3759–3763.
[6] L. Qiu, S.A. Pabit, A.E. Roitberg, and S.J. Hagen, *Smaller and faster: The 20-residue Trp-cage protein folds in 4 micros*, J. Am. Chem. Soc. 124 (2002), pp. 12952–12953.
[7] R. Zhou, *Trp-cage: Folding free energy landscape in explicit water*, Proc. Natl Acad. Sci. USA 100 (2003), pp. 13280–13285.
[8] A. Linhananta, J. Boer, and I. MacKay, *The equilibrium properties and folding kinetics of an all-atom Go model of the Trp-cage*, J. Chem. Phys. 122 (2005), 114901.
[9] C. Simmerling, B. Strockbine, and A.E. Roitberg, *All-atom structure prediction and folding simulations of a stable protein*, J. Am. Chem. Soc. 124 (2002), pp. 11258–11259.
[10] C.D. Snow, B. Zagrovic, and V.S. Pande, *The Trp cage: Folding kinetics and unfolded state topology via molecular dynamics simulations*, J. Am. Chem. Soc. 124 (2002), pp. 14548–14549.
[11] F. Ding, S.V. Buldyrev, and N.V. Dokholyan, *Folding Trp-cage to NMR resolution native structure using a coarse-grained protein model*, Biophys. J. 88 (2005), pp. 147–155.
[12] J. Juraszek and P.G. Bolhuis, *Sampling the multiple folding mechanisms of Trp-cage in explicit solvent*, Proc. Natl Acad. Sci. USA 103 (2006), pp. 15859–15864.
[13] D. Paschek, H. Nymeyer, and A.E. Garcia, *Replica exchange simulation of reversible folding/unfolding of the Trp-cage*

Downloaded At: 17:03 14 January 2011

miniprotein in explicit solvent: On the structure and possible role of internal water, J. Struct. Biol. 157 (2007), pp. 524–533.

[14] A. Schug, W. Wenzel, and U.H. Hansmann, *Energy landscape paving simulations of the Trp-cage protein*, J. Chem. Phys. 122 (2005), 194711.

[15] X. Wu and G. Narsimhan, *Coarse grain molecular dynamics simulation for the prediction of tertiary conformation of lysozyme adsorbed on silica surface*, Mol. Simul. 35 (2009), pp. 974–985.

[16] Y. Sugita and Y. Okamoto, *Replica-exchange molecular dynamics method for protein folding*, Chem. Phys. Lett. 314 (1999), pp. 141–151.

[17] D.A. Case, T.A. Darden, T.E. Cheatham III, C. Simmerling, J. Wang, R.E. Duke, R. Luo, K.M. Merz, B. Wang, D.A. Pearlman, M. Crowley, S. Brozell, V. Tsui, H. Gohlke, J. Mongan, V. Hornak, G. Cui, P. Beroza, C. Schafmeister, J.W. Caldwell, W.S. Ross, and P.A. Kollman, *AMBER 8*, University of California, San Francisco, CA, 2004.

[18] J. Wang, R.M. Wolf, J.W. Caldwell, P.A. Kollman, and D.A. Case, *Development and testing of a general AMBER force field*, J. Comput. Chem. 25 (2004), pp. 1157–1174.

[19] H.J.C. Berendsen, J.P.M. Postma, W.F.V. Gunsteren, A. DiNola, and J.R. Haak, *Molecular dynamics with coupling to an external bath*, J. Chem. Phys. 81 (1984), pp. 3684–3690.

[20] J.W. Pitera and W. Swope, *Understanding folding and design: Replica-exchange simulations of "Trp-cage" miniproteins*, Proc. Natl Acad. Sci. USA 100 (2003), pp. 7587–7592.

[21] W.C. Still, A. Tempczyk, R.C. Hawley, and T. Hendrickson, *Semianalytical treatment of solvation for molecular mechanics and dynamics*, J. Am. Chem. Soc. 112 (1990), pp. 6127–6129.

[22] D. Qiu, P.S. Shenkin, F.P. Hollinger, and W.C. Still, *The GB/SA continuum model for solvation. A fast analytical method for the calculation of approximate Born radii*, J. Phys. Chem. A 101 (1997), pp. 3005–3014.

[23] R. Zhou, *Free energy landscape of protein folding in water: Explicit vs. implicit solvent*, Proteins 53 (2003), pp. 148–161.

[24] R. Zhou, G. Krilov, and B.J. Berne, *Comment on "Can a continuum solvent model reproduce the free energy landscape of a beta-hairpin folding in water?" The Poisson–Boltzmann equation*, J. Phys. Chem. B 108 (2004), pp. 7528–7530.

[25] B. Hess, H. Bekker, H.J.C. Berendsen, and J.G.E.M. Fraaije, *LINCS: A linear constraint solver for molecular simulations*, J. Comput. Chem. 18 (1997), pp. 1463–1472.

[26] W. Humphrey, A. Dalke, and K. Schulten, *VMD: Visual molecular dynamics*, J. Mol. Graph. 14 (1996), pp. 33–38, 27–28.

Downloaded At: 17:03 14 January 2011